ATBD FLINT

Glint estimation in the NIR and SW infrared bands of MERIS and AATSR using AATSR measurements in the thermal infrared

Version 1.0

January 11, 2010

Rene Preusker
Juergen Fischer

January 11, 2010

Change log

09/01/2010 finalization

29/04/2009 thermal extrapolation

11/03/2009 changed the title, changed p_0 in the Gaussian approximation of the sun glint; added LUT interpolation; described the LUT creation in more detail; explained the ambiguity, included a change log, added a smal section "Nomenclature" to clarify the term *glint*; revised many sections

27/11/2008 First Version, very rough

Contents

0.1 Purpose of the document and objective

This document describes the algorithm for the estimation of the sea surface glint at MERIS channel 14 (880 nm) from AATSR measurements at 12µm, 11µm and 3.7µm. Some auxiliary data is needed, in particular i) the total amount of water vapor (see section 1.2.1.2), which is an operational product of the MERIS ground segment and ii) a cloud mask, which is part of the MERIS ground segment and of the AATSR ground segment. The glint estimation is consequently limited to cloud free pixel. The algorithm assumes, that MERIS and AATSR data is co-registered. The algorithm as well as this document is separated in two parts:

1. The calculation of the solar portion at AATSR 3.7µm by using the thermal radiance at AATSR 12µm and AATSR 11µm.
2. The geometrical conversion from AATSR observation geometry to MERIS observation geometry.

0.2 Nomenclature

In this document the term *glint* is defined as

$$\gamma := \frac{L}{E_0}$$

where L is the reflected *radiance* and E_0 the incomming *direct irradiance,* booth directly above the surface. The unit is sr^{-1}. This is different to the definiton of *reflectance*

$$\rho = \frac{L}{\cos(\vartheta_{in}) \cdot E_0}$$

which has the same unit! The *glint* in this document is a kind of *normalized radiance.* But it is a surface property, since the water body is assumed to be black and the atmosphere is empty.

1 Solar portion at 3.7µm

1.1 Algorithm Overview

The top of atmosphere radiance at AATSR channel at 3.7µm $L_{3.7}^{TOA}$ consists of reflected $L_{3.7}^{surf,S}$ and scattered $L_{3.7}^{scat,S}$ solar radiation as well as emitted radiation from the atmosphere $L_{3.7}^{atm,E}$ and the surface $L_{3.7}^{surf,E}$. $L_{3.7}^{TOA}$ can be written as:

$$L_{3.7}^{TOA} = L_{3.7}^{surf,E} + L_{3.7}^{surf,E} + L_{3.7}^{surf,S} + L_{3.7}^{scat,S} \tag{1.1}$$

For cloud free conditions the amount of molecular scattering is negligible ($\tau_{mol} < 0.00005$), the amount of aerosol scattering is very small and, compared to the amount of reflected and emitted radiation, negligible as well. (Under special conditions, in particular for high aerosol loadings due to desert outbreaks or for undetected clouds, this may be different, but it is not considered here). Therefore we can assume that $L_{3.7}^{scat,S} = 0$ and equation 1.1 simplifies to:

$$L_{3.7}^{TOA} = L_{3.7}^{surf,E} + L_{3.7}^{atm,E} + L_{3.7}^{surf,S} \tag{1.2}$$

With $L_{3.7}^{TOA,E} = L_{3.7}^{surf,E} + L_{3.7}^{atm,E}$, the top of atmosphere radiance without any solar radiation, as it is observed e.g. during night, the sum in equation 1.2 can be further simplified and the equation can be rearranged to:

$$L_{3.7}^{surf,S} = L_{3.7}^{TOA} - L_{3.7}^{TOA,E} \ . \tag{1.3}$$

The first objective is to find and calculate $L_{3.7}^{TOA,E}$ and to calculate therewith $L_{3.7}^{surf,S}$. This will be done by a linear regression of the thermal radiance of $L_{12}^{TOA,E}$ and $L_{11}^{TOA,E}$ to $L_{3.7}^{TOA,E}$.

The second objective is to correct $L_{3.7}^{surf,S}$ for water vapor transmission $T_{3.7}$ to obtain

the bottom of atmosphere glint $\gamma_{3.7}$.

$$\gamma_{3.7} = \frac{L_{3.7}^{surf,S}}{E_0 \cdot T_{3.7}} \tag{1.4}$$

or

$$\rho_{3.7} = \frac{L_{3.7}^{surf,S} \cdot \pi}{E_0 \cdot T_{3.7} \cdot cos\left(\vartheta_{sun}\right)} \cdot 100 \tag{1.5}$$

with the appropriate solar constant E_0 (integrated over the spectral response of AATSR 3.7µm and corrected for the specific solar earth distance) and the solar zenith angle ϑ_{sun}. The equations 1.4 and 1.5 are essentially the same, the first one has the unit $1/sr$ (eventually like the MERIS channels the second one the unit % (like the visible channels of AATSR). The calculation of the transmission $T_{3.7}$ will be done by using the water vapor content (which is an standard MERIS product) and appropriate weighted sums of mass extinction coefficients (see equation 1.12).

1.2 Algorithm Description

1.2.1 Theoretical description

1.2.1.1 Linear regression of 11µm and 12µm to 3.7µm

The thermal part of the radiance at 3.7µm channel will be calculated by the following simple linear regression:

$$BT_{3.7} = a + b \cdot BT_{11} + c \cdot (BT_{11} - BT_{12}) \tag{1.6}$$

The regression coefficients are:

$$a = 4.91348 \quad b = 0.978489 \quad c = 1.37919 \tag{1.7}$$

The coefficients have been found by analyzing cloud free sea surface night scenes. Figure 1.1 shows a scatter diagram of the regressed and the analysed night scenes. The rmse of the regression is 0.3K.

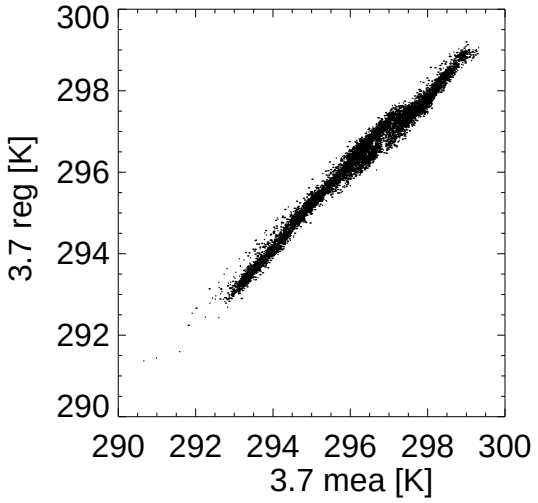

Figure 1.1: Scatter diagram of linear regression of 12µm and 12µm to 3.7µm.

The regression in equation 1.6 is in units of K, which is the elemental unit of the thermal channels, since they are calibrated using black-bodies. However the *intensive* quantity $BT^{3.7}$ must be converted into an *extensive* radiance to make the equations 1.1 - 1.5 applicable. This is done by a simple linear interpolation in the appropriate look up table LUT

$$L_{3.7}^{TOA,E} = LUT\left[BT_{3.7}\right] \tag{1.8}$$

1.2.1.2 Calculation of water vapor transmission

Generally a transmission T_λ through an air-mass m can be calculated as:

$$T_\lambda = exp\left(-m \cdot k_\lambda\right) \tag{1.9}$$

where $k_\lambda$is the mass extinction coefficient. This equation is only valid for constant extinction coefficients a) along the light path and b) along the spectral response of the receiver. Thus, in real world applications, equation 1.9 must be replaced by precise integrals over the spectral response and the atmospheric profiles of density, pressure and temperature. These integrals can be approximated by the following summations:

$$T = \sum_{i=1}^{n_i} w_i \left[\sum_{j=1}^{n_j} exp\left(-m \cdot k_{i,j}\right)\right] \tag{1.10}$$

where the atmosphere is separated in n_j layer and the spectral response can be pictured as divided into n_i not necessarily connected but homogeneous spectral intervals having the weight w_i. (details can be found in various publications describing the *k-distribution* e.g. Bennartz and Preusker, 2009). For solar radiation reflected on the bottom of a non-scattering atmosphere, the air-mass m is:

$$m = \frac{1}{cos\left(\vartheta_{sun}\right)} + \frac{1}{cos\left(\vartheta_{view}\right)} \ . \tag{1.11}$$

In this case $k_{i,j}$ is the absorption optical depth of layer j and interval i. The weights w_i and extinctions $k_{i,j}$ have been calculated for the AATSR 3.7µm channel using a k-binning technique for a mid-latitude standard atmosphere having a water vapor column of $wv_{MLS} = 2.7872\ g/cm^2$ and considering all other absorbing gases relevant for that channel. Hence the transmission of AATSRs channel at 3.7µm $T_{3.7}$ (which is needed in equations 1.4 and 1.5) is:

$$T_{3.7} = \sum_{i=1}^{n_i} w_i \left[\sum_{j=1}^{n_j} exp\left(-m \cdot \left(\frac{wv}{wv_{MLS}} \cdot k_{i,j}^{wv} + k_{ij}^{other} \right) \right) \right] \tag{1.12}$$

with wv the water vapor content, retrieved by MERIS's standard procedure or by other sources. To be flexible with the total amount of water vapor, the extinctions k_{ij} have been divided into the extinction due to water vapor k_{ij}^{wv} and the extinction due to other gases k_{ij}^{other}. k_{ij}^{wv} can then be scaled with a sufficient accuracy to the measured amount of water vapor.

1.2.1.3 Calculation of solar constant

$$r = 1 - 0.01673 \cdot cos\left(0.9856 \cdot (doy - 2)\right)$$

$$E_0 = \frac{E_0^{equinox}}{r^2}$$

with *doy* the day of year number.

1.2.1.4 Work flow summary

Eventually the calculation of the solar portion at 3.7µm is a sequence of the following steps (for details see sections 1.2.1.1 and 1.2.1.3):

1. Estimation of the thermal part at 3.7µm:

$$BT_{3.7} = a + b \cdot BT_{11} + c \cdot (BT_{11} - BT_{12}) \tag{1.13}$$

2. Conversions of brightness temperature to radiance:

$$L_{3.7}^{TOA,E} = LUT\left[BT_{3.7}\right] \tag{1.14}$$

3. Subtraction of the thermal signal from the top of atmosphere signal:

$$L_{3.7}^{surf,S} = L_{3.7}^{TOA} - L_{3.7}^{TOA,E} \tag{1.15}$$

4. Calculation of the atmospheric transmission at 3.7µm:

$$T_{3.7} = \sum_{i=1}^{n_i} w_i \left[\sum_{j=1}^{n_j} exp\left(-m \cdot \left(\frac{wv}{wv_{MLS}} \cdot k_{i,j}^{wv} + k_{ij}^{other} \right) \right) \right] \tag{1.16}$$

5. Correction of the atmospheric transmission:

$$\gamma_{3.7} = \frac{L_{3.7}^{surf,S}}{E_0 \cdot T_{3.7}} \tag{1.17}$$

2 Geometrical conversion

2.1 Algorithm Overview

The main objective of the of the *geometrical conversion* is the calculation of the glint at 0.885µm $\gamma_{0.88}$ from the glint at 3.7µm $\gamma_{3.7}$. Both values are not equal because i) the refractive index of water is different at both wavelengths and more important and more difficult to solve ii) the azimuth difference of the AATSR observation at 3.7µm is different to the azimuth difference of the MERIS observation.

The main quantity in the *geometrical conversion* is the *effective wind-speed* ws. It is assumed that there exists a unique relationship CM between the glint γ_λ at a specific wavelength λ, the observation geometry (ϑ_{sun}, ϑ_{view}, ϕ_{diff}), the refractive index of sea water at that wavelength n_λ and the wind-speed ws.

$$\gamma_\lambda = CM\left(\vartheta_{sun}, \vartheta_{view}, \phi_{diff}, n_\lambda, ws\right) \tag{2.1}$$

But studies have shown, that this relation does not exist, at least not precisely. In particular the wind direction, existing (cross) swell and the history of the waves and foam modulate the relationship and lead to different parametrization of sea surface roughness (Cox and Munk 1954, Ebuchi anfd Kizu 2002, Koepke 1984). However, as it will be shown later, the precise estimation of the wind-speed is *not* of interest. The task of the wind-speed ws is solely to act as a *consistent* parameter for the sea surface glint.

Since ws is the only unknown in the upper equation 2.1, there could be an unique inverse:

$$ws = CM^{-1}\left(\vartheta_{sun}, \vartheta_{view}, \phi_{diff}, n_\lambda, \gamma_\lambda\right) \tag{2.2}$$

Under the assumption that the unique inverse CM^{-1} exists, the geometrical conversion is straight forward and consists of the following two steps:

1. Calculation of the effective wind-speed ws

$$ws = CM^{-1}\left(\vartheta_{sun}, \vartheta_{view}, \phi_{diff}^{AATSR}, n_{3.7}, \gamma_{3.7}\right) \tag{2.3}$$

using the glint $\gamma_{3.7}$ (chapter 1) at 3.7µm, the AATSR azimuth difference ϕ_{diff}^{AATSR} and the refractive index of sea water at 3.7µm.

2. Calculation of the glint $\gamma_{0.88}$

$$\gamma_{0.88} = CM\left(\vartheta_{sun}, \vartheta_{view}, \phi_{diff}^{MERIS}, n_{0.88}, ws\right) \tag{2.4}$$

using the effective wind-speed ws from step 1, the MERIS azimuth difference ϕ_{diff}^{MERIS} and the refractive index of sea water at 0.88µm.

The forward operator CM in equations 2.1 and 2.4 is implemented and approximated by an two dimensional Gaussian function. The inverse operator CM^{-1} could not be approximated by an analytic function, because under some conditions/geometries it is not unique, but twofold (two effective wind-speeds can produce the same sun glint, Figure 2.3). Instead a simple and fast search algorithm was was implemented, that could give the possible wind-speeds (sections 2.2.1.1 - 2.2.1.4)

2.2 Algorithm Description

2.2.1 Theoretical description

2.2.1.1 CM: Gaussian approximation of sea surface glint

General Remark: It is of course possible to use a full RTM to calculate the sea surface glint based on the probability density function of the normals of the sea surface facets, as described by e.g. Cox and Munk. But this would be *i)* much to slow and *ii)* not feasible in any kind of ground segment or in BEAM. For this reason we utilized a two dimensional Gauss function to approximate the glint.

The observation angles have to be transformed into Cartesian coordinates:

$$x = \cos\left(\frac{\pi}{2} - \vartheta_{view}\right) \cdot \sin\left(\phi_{diff}\right)$$

$$y = \cos\left(\frac{\pi}{2} - \vartheta_{view}\right) \cdot \cos\left(\phi_{diff}\right)$$

The new coordinates x and y where used with a two dimensional Gaussian function:

$$u = \left(\frac{x}{p_1}\right)^2 + \left(\frac{y - p_3}{p_2}\right)^2$$

$$\gamma = \exp\left(p_0\right) \cdot \exp\left(\frac{-u}{2}\right) \tag{2.5}$$

to calculate the sea surface glint.

The needed parameter p_0, p_1, p_2 and p_4 have to be calculated from the sun zenith, the wind-speed and the refractive index of seawater. This is done by using a look up table (LUT). Eventually the LUT contains entries for the following transformation:

$$[ws, n_\lambda, \vartheta_{sun}] \implies [p_0, p_1, p_2, p_3] \tag{2.6}$$

but only on discrete points. The needed interpolation is realized within the table:

$$\forall_i : p_i = INT\_LUT_i\left(ws, n_\lambda, \vartheta_{sun}\right) \tag{2.7}$$

2.2.1.2 Generation of a look up table of Gaussian Cox and Munk parameter

The LUT was generated and filled using radiative transfer (MOMO) calculations for 15 different wind-speeds (1,...,15) m/s, 11 different refractive indices (1.30,...,1.40) and 13 solar zenith angles (0°,...,70°), leading to 2145 entries. The parameters $[p_0, p_1, p_2, p_3]$ of each entry have been estimated by a Levenberg-Marquard-Least-Square-Fit to minimize ϵin equation 2.8:

$$\epsilon = \sum^{\vartheta_{view}} \sum^{\phi_{diff}} \left[RTM\left[ws, n_\lambda, \vartheta_{sun}\right]\left(\vartheta_{view}, \phi_{diff}\right) - CM\left[p_0, p_1, p_2, p_3\right]\left(\vartheta_{view}, \phi_{diff}\right)\right]^2 \tag{2.8}$$

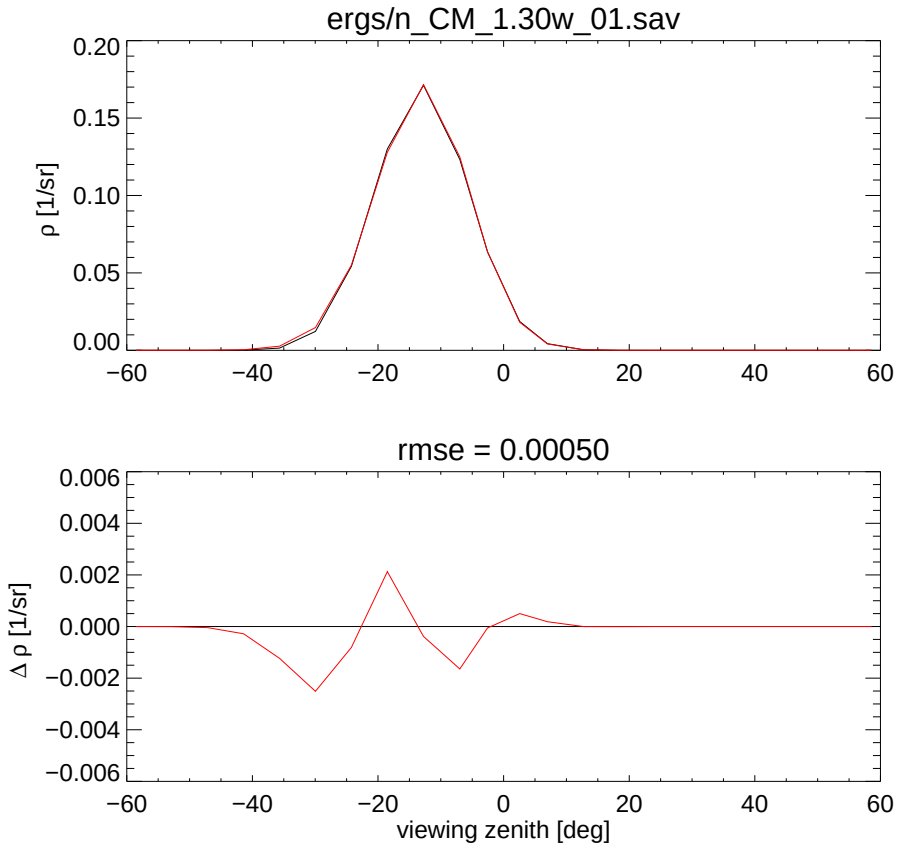

Figure 2.1: Example for the glint in the principle plane as calculated with MOMO (black) and fitted using the 2d Gaussian (red)

Figure 2.1 shows exemplary the glint in the principle plane as calculated with MOMO and fitted using the 2D Gaussian. Figure 2.2 illustrates the dependency of the parameter p_i from wind-speed, refractive index and sun zenith.

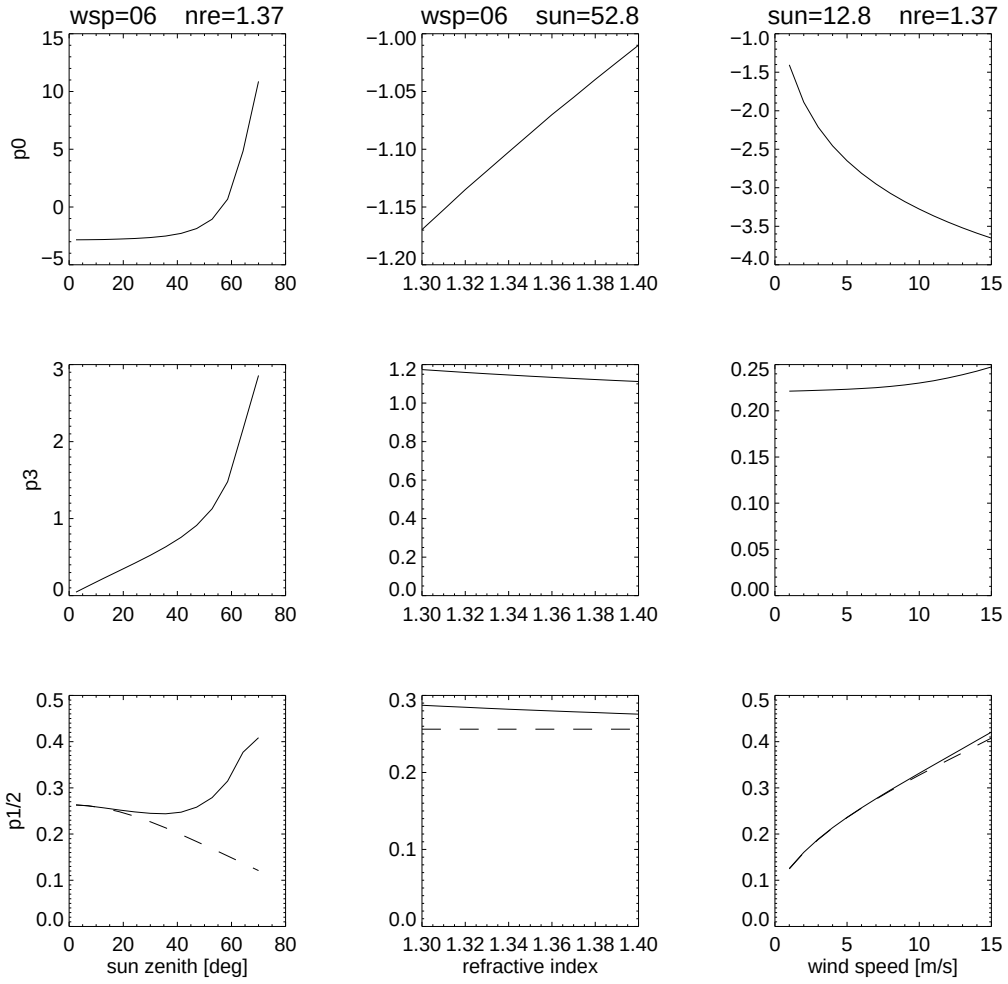

Figure 2.2: Dependency of the Gaussian parameters (p_0 upper row, p_3 middle row, p_1 and p_2 lower row) from sun zenith (left column), refractive index (middle column) and wind speed (right column).

Actually all known glint properties can be found:

1. p_0 which is mainly the amplitude of the glint, depends on ws, n_λ and ϑ_{sun} comparably.
2. p_3 which is the position of the maximum, depends especially on the sun zenith and slightly on the wind-speed.
3. p_1 and p_2, which are the width of the glint in the principal plane and across the principal plane, depend on wind-speed and sun zenith. For high sun elevations both widths are almost equal. For low sun positions the across principal plane

width is smaller than the along principal plane width.

However, the most important finding is that all parameter are continuous with respect to ws, n_λ and ϑ_{sun} and therewith a multi-dimensional regression or a linear interpolation is reasonable.

2.2.1.3 Retrieval of the Gaussian parameter using three-linear interpolation

Alternatively to the artificial neural network a direct LUT interpolation has been implemented to relate wind-speed ws, refractive index n_λ and sun zenith angle to the Gaussian parameter $[p_0, p_1, p_2, p_3]$:

$$\forall_i : p_i = INT\_LUT_i\left(ws, n_\lambda, \cos\left(\vartheta_{sun}\right)\right) \tag{2.9}$$

The interpolation is three dimensional linear and consists of the following steps.

1. Normalization of the input variables:

$$\tilde{ws} = \frac{ws - ws_l}{ws_{up} - ws_l} \tag{2.10}$$

   where ws_l and $ws_u$is the nearest lower and nearest upper wind-speed entry in the look up table. The refractive index and the sun zenith are normalized alike to retrieve $\tilde{n_\lambda}$and $\tilde{\vartheta}$.

2. Calculate the parameter $[p_0, p_1, p_2, p_3]$ by a weighted sum of the $2^3 = 8$ enveloping neighbors in the corresponding look up table:

$$\begin{aligned} \forall_i : \quad p_i &= (1-\tilde{ws})\,(1-\tilde{n_\lambda})\left(1-\tilde{\vartheta}\right) p_i^{l,l,l} \\ &+ (0+\tilde{ws})\,(1-\tilde{n_\lambda})\left(1-\tilde{\vartheta}\right) p_i^{u,l,l} \\ &... \\ &+ (0+\tilde{ws})\,(0+\tilde{n_\lambda})\left(0+\tilde{\vartheta}\right) p_i^{u,u,u} \end{aligned} \tag{2.11}$$

2.2.1.4 CM^{-1}: Retrieval of the effective wind-speed

As already mentioned, the effective wind-speed at a pixel can not be retrieved from the sea surface glint using an analytic function, regression etc. The reason is, that under some geometries one sea surface glint can belong to two very different wind-speeds . To overcome the ambiguity the following algorithm is used.

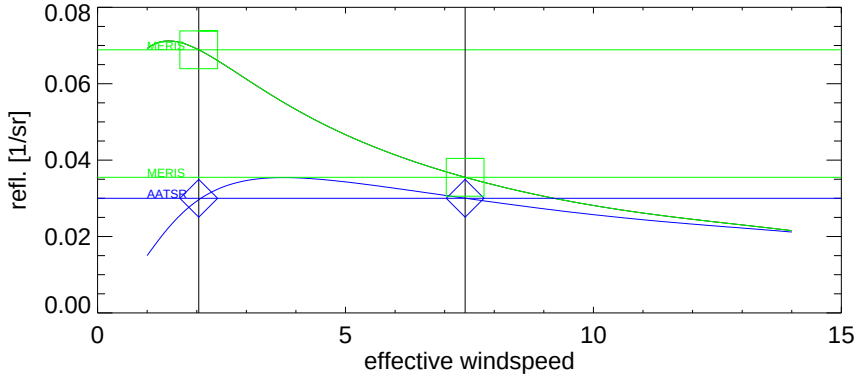

Figure 2.3: Sun glint (using the Cox and Munk parametrization) of MERIS ($\lambda = 0.88\mu m$, n=1.33, $\phi_{diff} = 30^o$) and AATSR ($\lambda = 3.7\mu m$, n=1.36, $\phi_{diff} = 10^o$) for a sun zenith of 30^o and a viewing zenith of 20^o as a function of wind-speed. An AATSR glint of 0.03 (blue horizontal line) could belong to two wind-speeds: 7.3 m/s and 2.1 m/s (two black vertical lines), and accordingly to two MERIS glints of 0.036 and 0.068 (the two green horizontal lines).

1. Generate at run time a small look up table LUT_{RHO} of sun glints for the actual AATSR sun and viewing geometry, the refractive index of sea water at 3.7µm, and 151 (this number is currently implemented, but may change) different wind-speeds between 1m/s and 15m/s. This is done by using equations 2.5 and **??**
2. Calculate the maximum absolute difference between two consecutive LUT_{RHO} elements
$$\Delta_{max} = \max_{\forall_i} \left(|LUT^i_{rho} - LUT^{i+1}_{rho}| \right)$$
3. Find the maximum in LUT_{rho}
$$\gamma_{max} = \max \left(LUT_{rho} \right)$$
4. If γ_{max} is not the first or last entry in the look up table, divide the table into two tables at the wind-speed belonging to $\gamma_{max}$and execute the following steps for booth tables.
5. Find the smallest absolute difference between $\gamma_{3.7}$ and the elements of the look up table(s) Δ_γ.
6. If Δ_γ is smaller than Δ_{max} take the corresponding wind-speed as a solution.

This algorithm can produce zero, one or two solutions. Two solutions results, if the look up table has a maximum and in booth branches a valid entry is found. One solution is found, if the look up table has only one branch and one valid entry, or if the look up table has two branches and but only one branch with a valid entry. It has zero solutions, if no valid entry is found (or the absolute difference between $\rho_{3.7}$ and the look up table elements is always larger than Δ_{max})

2.2.1.5 Handling of ambiguity

As shown, the inverse operator CM^{-1}can retrieve under some circumstances two wind-speeds. To overcome this ambiguity one of the wind-speeds have to be chosen. Two criteria have been investigated: i) take the one which is closer to ECMWF and ii) take the one which is closer to the local median. A third and probably best possibility is to dispose the decision subsequent algorithms (like aerosol remote sensing).

2.2.1.6 Work flow summary

Eventually the conversion of the sun glint from AATSR azimuth difference and refractive index at 3.7µm a sequence of the following steps:

1. Estimation of zero, one or two effective wind-speeds ws as described in section 2.2.1.4 using the inverse operator CM^{-1}:

$$ws = CM^{-1}(\vartheta_{sun}, \vartheta_{view}, \phi_{diff}^{AATSR}, n_{3.7}, \gamma_{3.7}) \tag{2.12}$$

2. If no wind-speed is found, consider the pixel as cloud (or something else) contaminated
3. If two wind-speeds are found choose the most likely as described in section 2.2.1.5.
4. Calculate from the effective wind-speed ws, the observation geometry of MERIS and the refractive index of sea water at 0.88µm the corresponding sun glint using the forward operator CM described in section 2.2.1.1:

$$\gamma_{0.88} = CM\left(\vartheta_{sun}, \vartheta_{view}, \phi_{diff}^{MERIS}, n_{0.88}, ws\right)$$

3 Example

An example for the application of the FLINT algorithm is given in Figure 3.1.

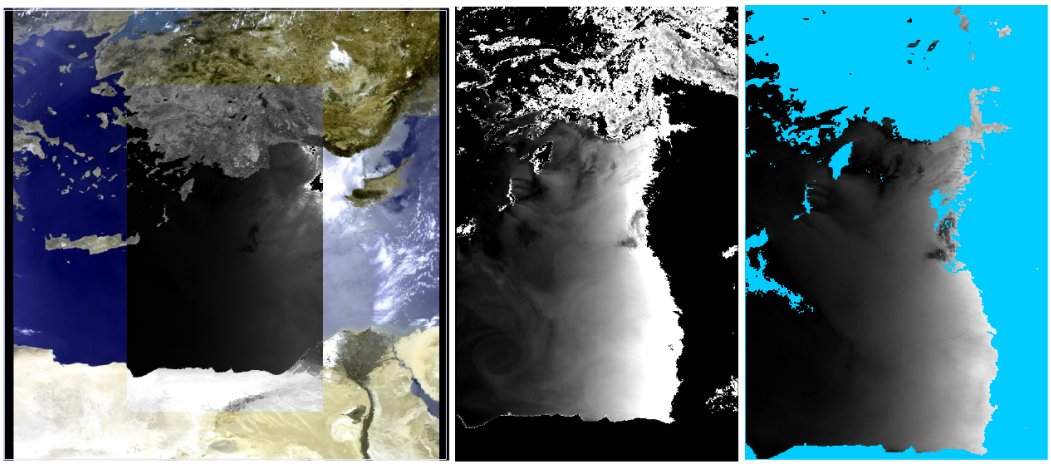

Figure 3.1: From left to right. 1.) True colour composite of a glint affected scene of the Mediterranean on the 13.Jun 2003observed by MERIS and a black white overlay of AATSR 1.6µm nadir view. 2.) The same scene measured by AATSR 3.7µm. Due to the high reflectivity of the glint and some land surfaces this channel is partly saturated. AATSR: 3.) The estimated sea surface glint at 0.885µm for the MERIS viewing geometry.

4 Practical considerations

4.1 Numerical computation consideration

None

4.2 Programming considerations

The algorithm is implemented in BEAM.

4.3 Quality control

Validation is ongoing.

4.4 Exception handling

None yet. Desert outbreak events have to be flaged and to be handled differently in future.

4.5 Error budget estimates

Source of errors:

1. Inaccuracy of regression from 11µm and 12µm to 3.7µm. The estimated accuraccy is 0.3K (rmse). This error is comparably small, less than 1% for high glint.
2. Inaccuraccy of the used water vapor. The used MERIS water vapor is not validated yet. We know that over ocean errors of up to 30% of the water vapor estimates can occur. This translates into an error of transmission of up to 15% , depending on air mass.

3. Inacurate co-location of AATSR and MERIS. The impact of the colocation error is not yet be estimated, however, a high number of sceenes has to be analysed for that.
4. Undetected clouds will lead to a high reflectance at 3.7µm, which is not related to a glint pattern. A high number of sceenes has to be analysed for quantification.
5. Non-uniform wind speeds or glint patterns within a pixel. The effects have not been studied so far. We propose to quantify the probability of occurence using ENVISAT SAR data, and to estimate the significance by independent pixel aproximations with radiative transfer simulations.

4.6 Auxiliary data

1. Spectral refrective index of water.
2. Atmospheric transmission of water vapor and other gases.
3. AATSR 3.7µm BT to radiance calbration table.
4. Look up tables for sea surface roughness model (equation 2.6).

References

Cox, C. and W. H. Munk, (1954): Statistics of the sea surface derived from sun glitter. J. Mar. Res., 13, 198–227.

Cracknell, A.P., (1993): A method for the correction of sea surface temperature derived from satellite thermal infrared data in an area of sunglint, Int. J. Remote Sensing, 14.

Ebuchi, N. and S. Kizu, (2002): Probability Distribution of Surface Wave Slope Derived Using Sun Glitter Images from Geostationary Meteorological Satellite and Surface Vector Winds from Scatterometers, Journal of Oceanography, Vol. 58, pp. 477 to 486.

Fell F, Fischer J, (2001): Numerical simulation of the light field in the atmosphere-ocean system using the matrix- operator method. J QUANT SPECTROSC RA 69 (3): 351-388.

Koepke, P., (1985): The reflectance factors of a rough ocean with foam-comment on 'Remote sensing of the sea state using the 0'8-1'1 /lm spectral band' by L. Wald and J. M. Monget, Int. J. Remote Sensing, 1985, VOL. 6, No.5, 787-799.